Grant/Contract Title: (YIP-08) EXPLORATORY PHASE TRANSITION-BASED
SWITCHES USING FUNCTIONAL OXIDES
Grant/Contract Number: FA9550-08-1-0203

PI: Shriram Ramanathan[*]

*School of Engineering and Applied Sciences, Harvard University, Cambridge, Massachusetts
02138*

[*] *shriram@seas.harvard.edu*

TECHNICAL REPORT

Abstract

Vanadium dioxide (VO_2) undergoes a sharp metal-insulator transition (MIT) in the vicinity of
room temperature and there is great interest in exploiting this effect in novel electronic and
photonic devices. We have measured the work function of VO_2 thin films across the phase
transition for the first time using variable temperature Kelvin force microscopy (KFM). The
work function of VO_2 is estimated to be ~ 5.15 eV in the insulating phase and increases by ~
0.15 eV across the MIT. We further show that the work function change upon the phase
transition is highly sensitive to near-surface stoichiometry studied by X-ray photoelectron
spectroscopy. The results are pertinent to understanding fundamental electronic properties of
vanadium oxide as well as charge injection phenomena in solid state devices incorporating
complex oxides containing multi-valent cations.

1. REPORT DATE **02 FEB 2011**	2. REPORT TYPE	3. DATES COVERED **00-00-2010 to 00-00-2011**

4. TITLE AND SUBTITLE **Exploratory Phase Transition-Based Switches Using Functional Oxides**	5a. CONTRACT NUMBER
	5b. GRANT NUMBER
	5c. PROGRAM ELEMENT NUMBER
6. AUTHOR(S)	5d. PROJECT NUMBER
	5e. TASK NUMBER
	5f. WORK UNIT NUMBER

7. PERFORMING ORGANIZATION NAME(S) AND ADDRESS(ES) **Harvard Univ,Cambridge,MA,02138**	8. PERFORMING ORGANIZATION REPORT NUMBER **; AFRL-OSR-VA-TR-11-056**

9. SPONSORING/MONITORING AGENCY NAME(S) AND ADDRESS(ES)	10. SPONSOR/MONITOR'S ACRONYM(S)
	11. SPONSOR/MONITOR'S REPORT NUMBER(S) **AFRL-OSR-VA-TR-11-056**

12. DISTRIBUTION/AVAILABILITY STATEMENT
Approved for public release; distribution unlimited

13. SUPPLEMENTARY NOTES

14. ABSTRACT

15. SUBJECT TERMS

16. SECURITY CLASSIFICATION OF:			17. LIMITATION OF ABSTRACT	18. NUMBER OF PAGES	19a. NAME OF RESPONSIBLE PERSON
a. REPORT **unclassified**	b. ABSTRACT **unclassified**	c. THIS PAGE **unclassified**	**Same as Report (SAR)**	**13**	

The mechanisms governing metal-insulator transition (MIT) in vanadium dioxide (VO_2) is an intensively explored subject in condensed matter sciences.[1] While electron-electron interactions leading up to the Mott interaction may cause the transition, structural transformation which occurs concurrently with MIT at ~ 340 K opens another possibility, Peierls instability.[2-3] The phase structure of VO_2 changes from rutile to monoclinic under cooling accompanied by cell size doubling and tilted V-V pair formation, possibly leading to band gap opening.[3] There is substantial technological interest in exploiting the ultrafast phase transition in advanced electronics and optoelectronics.[4-7] It is to be noted however that the elementary electronic properties of VO_2 such as intrinsic carrier concentration, work function, and dielectric properties in thin film structures have not yet received much attention.[8] The existence of multiple valence states of V complicates the material chemistry and in particular controlling surface stoichiometry is of paramount importance.[9] Surfaces may contact electrodes and hence affect barriers for charge injection, and in many devices, the near-surface regions may serve as channel layers and carrier concentration is of critical importance. The work function, Φ, defined as an amount of energy required to extract an electron from Fermi energy level of material surface to vacuum is crucial to design electronic devices such as metal-oxide junctions and field-effect devices.[10] Also by measuring Φ across transition boundary, the surface phase transition characteristics can be studied.[11] Kelvin force microscopy (KFM) has been used to investigate Φ variation driven by MIT on the surface of VO_2 thin films in this work for the first time.

In this letter, we report Φ values of VO_2 as a function of temperature spanning the phase transition. Also, we observed two important facts by systematic temperature-variable KFM studies along with detailed conduction transport measurements and X-ray photoelectron spectroscopy (XPS): 1) Φ of VO_2 film surface increases with raising temperature, T, across phase boundary and 2) the phase transition characteristics in the near-surface region of VO_2

films are clearly differentiated from those of VO_2 film bulk due to stoichiometry variation from surface to film interior. In addition, it was also observed that the degree of MIT-induced variation in both Φ and σ of VO_2 films are substantially affected by oxygen stoichiometry.

Highly textured vanadium dioxide films were grown on single crystal Al_2O_3 (0001) substrates by RF-sputtering from a VO_2 target (99.5%, AJA International Inc.). During synthesis, the substrate temperature and RF-source power were set as 550°C and 150 W respectively. The process gas pressure was kept at 10 mTorr using Ar and oxygen gas mixture whose oxygen content was controlled in detail to prepare a set of VO_2 samples of different oxygen stoichiometry. For this work, three representative samples (thickness ~ 200nm) deposited with oxygen content of ~ 1.75%, ~ 1.25%, and ~ 1.10% were chosen and labeled as A, B, and C respectively henceforth. The resistivity, ρ, of VO_2 films was measured varying T on the devices where VO_2 films are patterned by photolithography and Cr/Au electrodes are coated by thermal evaporation using four-probe methods in an environmental probe station equipped with a heating stage whose T is calibrated with thermocouples carefully. In-depth XPS profiling was performed on SSX-100 ESCA XPS system using Al $K\alpha$ x-ray source (1.4866 keV) and Ar ion sputtering in ultra-high vacuum condition.

KFM was performed using Pt-coated conducting tips (MikroMasch DPER14) on Asylum MFP-3D atomic force microscopy (AFM) system including a heating stage module in the T range from 300 K to 368 K in the ambient environment. KFM is a scanning probe microscopy technique to measure contact potential difference (CPD) and topography simultaneously with a high lateral resolution (< 50 nm) as well as a high CPD sensitivity (< 0.1 mV).[12] One of the benefits of KFM technique over other area-averaged methods such as photoemission spectroscopy is that accurate Φ measurement is enabled by selective scanning.[13] Also, the high resolution of CPD and spatial dimension make it possible to estimate the work function of nano-scale features.[14] As a control for our measurement

reported in this letter, a Si-based reference structure was tested and the accuracy of Φ was estimated as ~ 0.02 eV.[13] 30 nm-thick Au/Cr layer including windows of 2×0.2 mm^2 was coated on VO$_2$ films and used as grounded reference for Φ calibration. The samples were cleaned with acetone (ultrasonic) and isopropyl alcohol prior to measurements. To estimate Φ of VO$_2$, CPD was scanned across the interface between the reference Au surface and the uncoated VO$_2$ film region. The scan region has a rectangular shape of 24×1.5 μm^2 size for full saturation of CPD in both sides. The tip height from the surface was maintained to be 15 nm. At each T, KFM scans were conducted continuously for at least 4~5 hours until the thermal drift is eliminated and surface potential is stabilized.

By measuring ρ as a function of T spanning the transition regime, the MIT characteristics of bulk region of VO$_2$ films can be investigated since the measured ρ is mostly determined by the conductance of bulk of the film. The ρ vs. T plots measured from the samples A-C are summarized in fig. 1 with an inset including the schematic image of the patterned device for electrical transport characterization by four terminal measurements. Sample A shows a sharp transition with the largest resistivity ratio of four orders via transition to metallic phase indicating that the average nominal film stoichiometry is closest to that of VO$_2$. On the other hand, the transition in sample B is relatively less sharp and with a lower transition temperature indicating that sample B includes more portion of phases of lower oxidation states as compared with sample A.[9] Sample C is observed to have only metallic characteristic in the whole T range without evident transition. This trend is to be expected considering that sample A was grown with optimal gas configuration and others are prepared in more reduced environment intentionally.

Each line scanning of KFM mode is composed of a topography scan and a subsequent CPD measurement. The measured CPD on Au (left) and VO$_2$ (right) side are equal to (Φ_{tip} − Φ_{Au})/e and (Φ_{tip} − Φ_{VO2})/e respectively and hence the Φ difference between Au and VO$_2$, Φ_{Au}

$- \Phi_{VO2}$, can be converted from CPD between Au and VO$_2$. Fig. 2 shows a surface topography map (a) and a series of CPD images ((b) to (e)) obtained by scanning the same area of sample A varying temperature along with the corresponding histograms to each CPD map in (f). The topography map was flattened by 0th order polynomial and the CPD scan images were rescaled setting the positions of the all histogram peaks corresponding to CPD on Au region same as that at 300 K due to the slight fluctuation of surface potential. From the distance of two peak positions in the histogram (i.e. CPD between Au and VO$_2$), we can extract Φ_{VO2} using the reported Φ_{Au} value of 5.10 eV [15]. Surprisingly, the Φ_{VO2} of sample A surface is almost constant ~ 5.17~5.18 eV regardless of T though the sharp transition was verified in terms of ρ representing film bulk properties. This result represents that the phase transition does not necessarily occur in the surface region of sample A due to the existence of more oxidized phase. This will be discussed further later. The contrast of KFM resembling grain structures is likely due to the existence of different stoichiometric phases along grain boundaries rather than the topographical effect as also observed by conductive AFM.[16]

On the other hand, as displayed in fig. 3 (b) to (e), slightly oxygen-deficient sample B shows a significant change in Φ_{VO2} as T increases. This can be seen clearly in the set of histograms displayed at varying temperature in fig 3 (f), Φ_{VO2} of sample B is observed to increase by ~ 0.15 eV via MIT under heating representing the major phase near the surface is VO$_2$ and the Fermi energy level, E_F, is shifted down with respect to vacuum due to the metallic phase formation. In the case of sample C (KFM images not shown), the increase of Φ is smaller as ~ 0.08 eV over the same temperature range indicating the fraction of VO$_2$ phase on sample C surface is relative lower than that on sample B surface. Though sample A shows better MIT properties of the bulk film, in terms of both morphology and surface MIT functionality, sample B could be more interesting for VO$_2$-based devices such as a field-effect transistor where primarily the properties of narrow channel region beneath surface are critical

for device performance.[7] This would be extremely important synthesis-related knowledge for VO$_2$ devices.

The band structure of both monoclinic and rutile VO$_2$ phases has been explored by photoemission studies[17-19] as well as theoretical calculations.[20-21] Accordingly, the change of Φ driven by MIT is discussed using the energy band diagram.[7,17,22] The Φ of metallic rutile VO$_2$ phase, Φ_M, equals to the ionization energy of metal phase, E_M, while Φ of insulating monoclinic VO$_2$ phase, Φ_I, is expressed by $\Phi_I = E_I + \Delta E_c$ where E_I is the ionization energy of insulator phase and ΔE_c is the energy difference between the bottom of conduction band and E_F. In a recent photoemission spectroscopy study on VO$_2$ films, ΔE_c was estimated to be $\sim$ 0.1 eV probably due to the existence of donor-like oxygen defects.[19] Therefore, using our results on sample B, the increase in ionization energy by the transition to metallic phase is estimated to be in the $E_M - E_I \sim 0.15$-0.25 eV range.

In fig. 4, Φ vs. T plots obtained from all samples are summarized. The inset shows the average Φ at 300 K (square) and 368 K (triangle) with error bars of standard deviation, which are calculated from a series of CPD measurements under repetitive heating cycles on different regions of devices. The small errors in Φ measurements indicate our KFM results are reproducible. By comparison with ρ data in Fig. 1 characterizing bulk film properties, we can clearly see the gap between MIT characteristics of surface and bulk-region of VO$_2$ films and such differences in surface and bulk transition characteristics in VO$_2$ has also been observed by scanning tunneling microscopy studies.[23] The gradual transition of Φ unlike the sharp jump of conductivity is likely caused by non-uniform stoichiometry near the film surface.

To understand this feature further, we conducted XPS measurements on the samples as a function of thickness. The O/V stoichiometry ratio was calculated with O$_{1s}$ and V$_{2p3/2}$ peaks of XPS profiles using CasaXPS software. As summarized in Fig. 5, the stoichiometry for the samples is observed to vary as a function of depth consistent with literature reports.[24] At the

surface, regardless of deposition conditions, the O/V stoichometry is close to 2.5 (V_2O_5 phase) and the O/V ratio decreases to ~ 1.8 with different decay rates depending on deposition conditions. Sample A grown with the highest oxygen content shows the slowest decrease rate in O/V ratio as a function of depth verifying the greater amount of VO_2 phase is present in sample A bulk than in the other samples. The off-stoichimetry in sample C verifies the poor MIT properties as observed in ρ measurements. To consider the chemical state near surface affecting the surface phase transition feature, the stoichiometry averaged over the Debye screening length of VO_2 (~ 5 nm)[7] is estimated by the first order exponential decay fitting and the calculated average O/V ratios of near-surface regions in samples A-C are ~ 2.4, ~ 2.2, and ~ 1.8 respectively. While the near-surface stoichiometry of sample A is close to that of V_2O_5 phase that does not undergo a metal-insulator transition, O/V ratios of the other samples are close to 2 (VO_2 phase). It is not surprising that the XPS analysis results of samples A-C match well with both corresponding Φ and ρ characteristics.

In summary, temperature-dependence of work function has been measured in VO_2 thin film surfaces by Kelvin force microscopy for the first time. The clear change in work function indicates that Fermi energy shift occurs during MIT resulting from the surface band structure changes upon the phase transition. By comparing work function and electric conductivity coupled with X-ray photoelectron spectroscopy studies, the importance of surface stoichiometry is clearly elucidated. The results are of relevance to understanding MIT phenomena in correlated oxide surfaces and highlight the role of surface chemistry in fabricating devices incorporating compositionally complex oxides.

Figure captions

Fig. 1. Resistivity vs. temperature plots measured from samples A-C were grown with

oxygen content of ~ 1.75%, ~ 1.25%, and ~ 1.10% respectively with an inset displaying the picture of device used for the four probe conductivity measurement.

Fig. 2. (a) 0th order flattened surface topography map and (b)-(e) contact potential difference (CPD) scan images at varying temperatures measured on the identical region of sample A with a set of histograms extracted from corresponding CPD maps in (b)-(e) respectively. The left half of scanned area is coated with ~ 30 nm-thick Au/Cr layer for work function reference on the VO_2 film.

Fig. 3. (a) 0th order flattened surface topography map and (b)-(e) contact potential difference (CPD) scan images at varying temperatures measured on the identical region of sample B with a set of histograms extracted from corresponding CPD maps in (b)-(e) respectively. The left half of scanned area is coated with ~ 30 nm-thick Au/Cr layer for work function reference on the VO_2 film.

Fig. (4) Work function vs. temperature plots measured from the surface of samples A-C with an inset of the average work function values with error bars representing standard deviation measured at 300 K and 368 K under repeated heating cycles on different scanned regions.

Fig. (5) The variation of O/V stoichimetry ratio of samples A-C as a function of depth from VO_2 film surface estimated by X-ray photoelectron spectroscopy. Two dashed lines indicate the O/V ratio of V_2O_5 (2.5) and VO_2 (2) phases.

References

(1)   Imada, M.; Fujimori, A.; Tokura, Y. Metal-insulator transitions. *Reviews of Modern Physics* **1998**, *70*, 1039.

(2)   Mott, N. F. Metal-Insulator Transition. *Reviews of Modern Physics* **1968**, *40*, 677.

(3)   Goodenough, J. B. The two components of the crystallographic transition in VO2. *Journal of Solid State Chemistry* **1971**, *3*, 490-500.

(4)   Newns, D. M.; Misewich, J. A.; Tsuei, C. C.; Gupta, A.; Scott, B. A.; Schrott, A. Mott transition field effect transistor. *Applied Physics Letters* **1998**, *73*, 780-782.

(5)   Guiton, B. S.; Gu, Q.; Prieto, A. L.; Gudiksen, M. S.; Park, H. Single-Crystalline Vanadium Dioxide Nanowires with Rectangular Cross Sections. *Journal of the American Chemical Society* **2004**, *127*, 498-499.

(6)   Hyun-Tak, K.; et al. Mechanism and observation of Mott transition in VO 2 - based two- and three-terminal devices. *New Journal of Physics* **2004**, *6*, 52.

(7)   Ruzmetov, D.; Gopalakrishnan, G.; Ko, C.; Narayanamurti, V.; Ramanathan, S. Three-terminal field effect devices utilizing thin film vanadium oxide as the channel layer. *Journal of Applied Physics* **2010**, *107*, 114516-114516-114518.

(8)   Yang, Z.; Ko, C.; Balakrishnan, V.; Gopalakrishnan, G.; Ramanathan, S. Dielectric and carrier transport properties of vanadium dioxide thin films across the phase transition utilizing gated capacitor devices. *Physical Review B* **2010**, *82*, 205101.

(9)   Griffiths, C. H.; Eastwood, H. K. Influence of stoichiometry on the metal-semiconductor transition in vanadium dioxide. *Journal of Applied Physics* **1974**, *45*, 2201-2206.

(10)   Neaman, D. A. *Semiconductor Physics and Devices*, 3rd ed.; Tata McGraw-Hill Publishing Ltd, 2007.

(11)   Kim, T.-H.; Angst, M.; Hu, B.; Jin, R.; Zhang, X.-G.; Wendelken, J. F.; Plummer, E. W.; Li, A.-P. Imaging and manipulation of the competing electronic phases near the Mott metal-insulator transition. *Proceedings of the National Academy of Sciences* **2010**, *107*, 5272-5275.

(12)   Nonnenmacher, M.; Oboyle, M. P.; Wickramasinghe, H. K. Kelvin probe force microscopy. *Applied Physics Letters* **1991**, *58*, 2921-2923.

(13)   Jaramillo, R.; Ramanathan, S. Kelvin force microscopy studies of work function of transparent conducting ZnO:Al electrodes synthesized under varying oxygen pressures. *Solar Energy Materials and Solar Cells* **2011**, *95*, 602-605.

(14)   Leendertz, C.; Streicher, F.; Lux-Steiner, M. C.; Sadewasser, S. Evaluation of Kelvin probe force microscopy for imaging grain boundaries in chalcopyrite thin films. *Applied Physics Letters* **2006**, *89*, 113120.

(15)   Michaelson, H. B. The work function of the elements and its periodicity. *Journal of Applied Physics* **1977**, *48*, 4729-4733.

(16)   Kim, J.; Ko, C.; Frenzel, A.; Ramanathan, S.; Hoffman, J. E. Nanoscale imaging and control of resistance switching in VO[sub 2] at room temperature. *Applied Physics Letters* **2010**, *96*, 213106.

(17)   Shin, S.; Suga, S.; Taniguchi, M.; Fujisawa, M.; Kanzaki, H.; Fujimori, A.; Daimon, H.; Ueda, Y.; Kosuge, K.; Kachi, S. Vacuum-ultraviolet reflectance and photoemission study of the metal-insulator phase transitions in VO_{2}, V_{6}O_{13}, and V_{2}O_{3}. *Physical Review B* **1990**, *41*, 4993.

(18)   Okazaki, K.; Wadati, H.; Fujimori, A.; Onoda, M.; Muraoka, Y.; Hiroi, Z. Photoemission study of the metal-insulator transition in VO_{2}/TiO_{2}(001): Evidence for strong electron-electron and electron-phonon interaction. *Physical Review B* **2004**, *69*, 165104.

(19)   Dmitry, R.; et al. Infrared reflectance and photoemission spectroscopy studies across the phase transition boundary in thin film vanadium dioxide. *Journal of Physics: Condensed Matter* **2008**, *20*, 465204.

(20)   Wentzcovitch, R. M.; Schulz, W. W.; Allen, P. B. VO_{2}: Peierls or Mott-Hubbard? A view from band theory. *Physical Review Letters* **1994**, *72*, 3389.

(21)   Gatti, M.; Bruneval, F.; Olevano, V.; Reining, L. Understanding Correlations in Vanadium Dioxide from First Principles. *Physical Review Letters* **2007**, *99*, 266402.

(22)   Qazilbash, M. M.; Burch, K. S.; Whisler, D.; Shrekenhamer, D.; Chae, B. G.; Kim, H. T.; Basov, D. N. Correlated metallic state of vanadium dioxide. *Physical Review B* **2006**, *74*, 205118.

(23)   Yin, W.; Wolf, S.; Ko, C.; Ramanathan, S.; Reinke, P. Nanoscale probing of electronic band gap and topography of VO[sub 2] thin film surfaces by scanning tunneling microscopy. *Journal of Applied Physics* **2011**, *109*, 024311-024318.

(24)   Lu, S.; Hou, L.; Gan, F. Surface analysis and phase transition of gel-derived VO2 thin films. *Thin Solid Films* **1999**, *353*, 40-44.
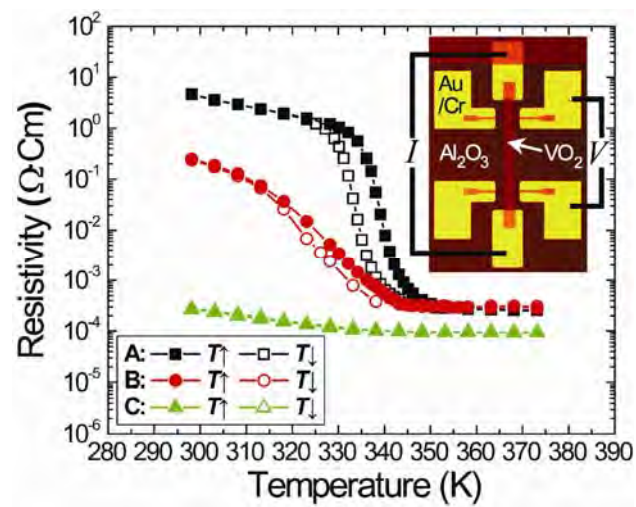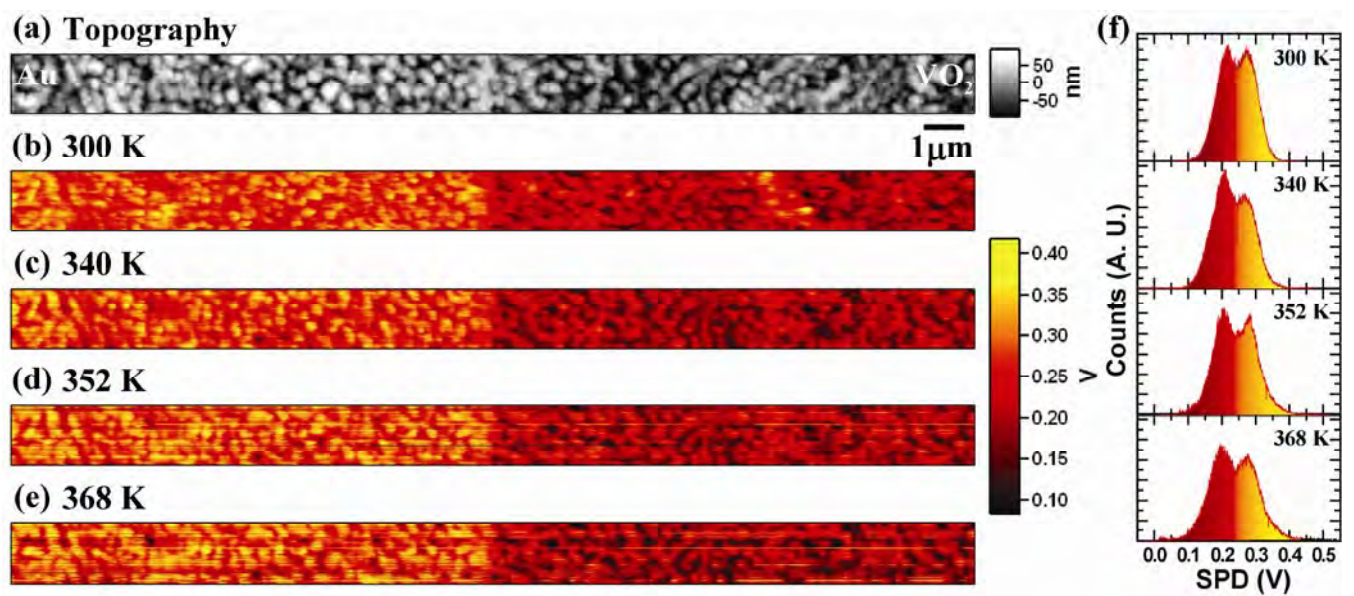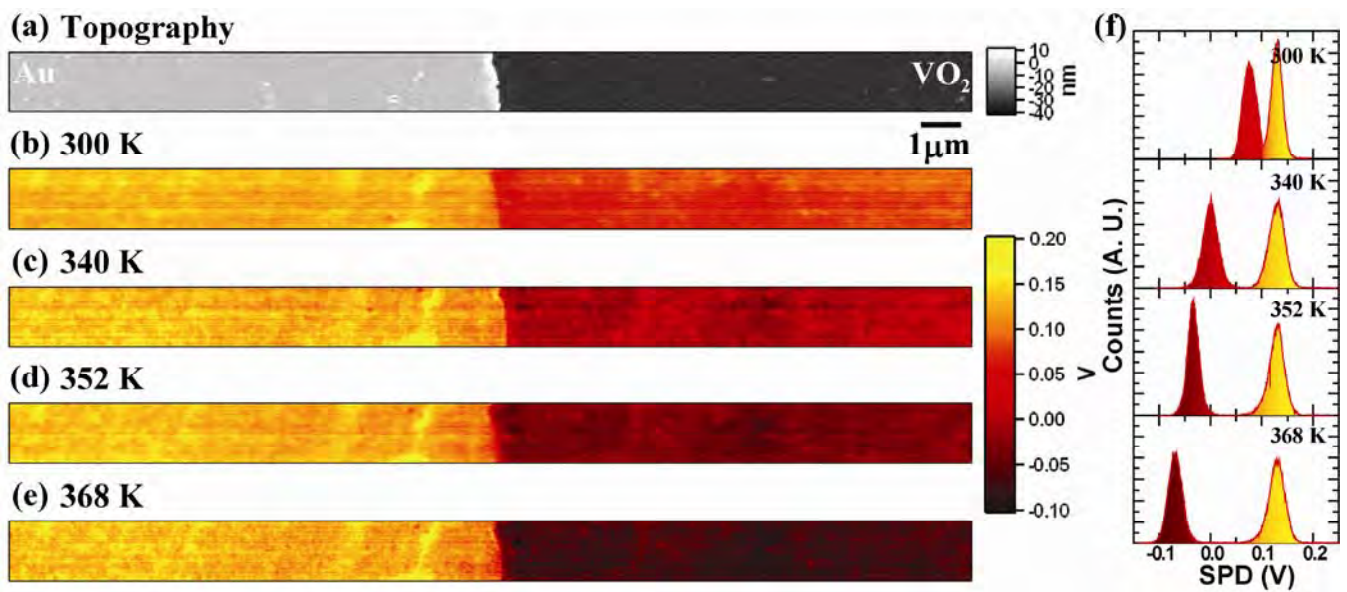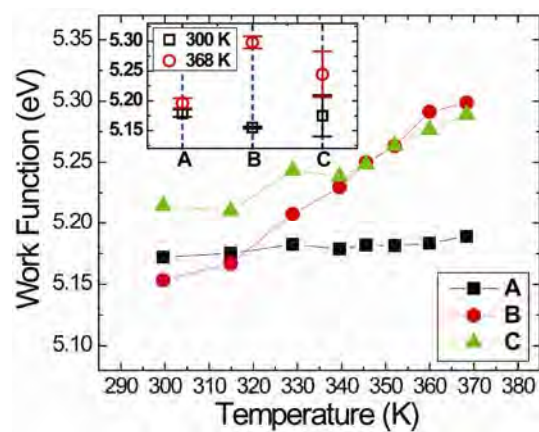
Fig. 1

Fig. 2

(a) Topography

(b) 300 K

(c) 340 K

(d) 352 K

(e) 368 K

(f)

Fig. 3

(a) Topography

Au

VO$_2$

1 µm

(b) 300 K

(c) 340 K

(d) 352 K

(e) 368 K

(f)

Fig. 4

Fig. 5